Investigating the Impact of Tool Type on Optimizing Burnishing Parameters for AISI 1035 Steel: A Taguchi and RSM Approach

Mahmoud Elsamanty [a,b], Waleed F. Youssef [c*], M. Abdelsalam [d], A.A. Ibrahim [a]

[a] Mechanical Engineering Department, Faculty of Engineering at Shoubra, Benha University, 108 Shoubra St., Cairo, Egypt.
[b] Mechatronics and Robotics Department, School of Innovative Engineering Design, Egypt-Japan University of Science and Technology (E-JUST), Alexandria, Egypt.
[c] Mechanical Engineering Department, Faculty of Engineering, Sinai University, Arish, North Sinai, Egypt.
[d] Department of Design and production engineering - faculty of Engineering – Ain Shams University, Cairo, Egypt.
* Corresponding Author.
E-mail: mahmoud.alsamanty@feng.bu.edu.e, mahmoud.elsamanty@ejust.edu.eg, waleed.mohammed@su.edu.eg, Mohamed.Abdelsalam@eng.asu.edu.eg, abdelkader.ibrahim@feng.bu.edu.eg

Abstract. Metal burnishing is a prominent surface finishing process that plays a significant role in enhancing surface quality. This research focuses on the optimization of ball burnishing process parameters using the Taguchi and Response Surface Methodology (RSM) approaches. The study employs three distinct tools designed for this purpose, with experiments conducted. Surface roughness and out-of-roundness measurements were performed. The Taguchi method demonstrated that the rigid tool achieved minimum surface roughness at a burnishing speed of 500 rpm, a feed rate of 0.09 mm/rev, and a penetration depth of 0.35 mm. Conversely, the pneumatic tool achieved the minimum surface roughness at a burnishing speed of 600 rpm, a feed rate of 0.1 mm/rev, and a penetration depth of 0.2 mm. Regarding out-of-roundness, the rigid tool achieved minimum values at a burnishing speed of 600 rpm, a feed rate of 0.11 mm/rev, and a penetration depth of 0.35 mm. For the pneumatic tool, the minimum value was yielded at a burnishing speed of 300 rpm, a feed rate of 0.09 mm/rev, and a depth of penetration of 0.2 mm. Furthermore, the Response Surface Methodology (RSM) revealed that the rigid tool achieved the minimum

surface roughness at a burnishing speed of 496.9697 rpm, a feed rate of 0.09 mm/rev, and a penetration depth of 0.35 mm. In contrast, the spring tool achieved the minimum surface roughness at a burnishing speed of 451.5152 rpm, a feed rate of 0.12 mm/rev, and a penetration depth of 0.35 mm. Regarding out-of-roundness, the rigid tool yielded the minimum values at a burnishing speed of 600 rpm, a feed rate of 0.12 mm/rev, and a penetration depth of 0.35 mm. The pneumatic tool achieved the minimum out-of-roundness at a burnishing speed of 300 rpm, a feed rate of 0.1006 mm/rev, and a penetration depth of 0.2 mm.

Keywords: Burnishing, Optimization, Taguchi, RSM.

1. INTRODUCTION

The precision and functionality of mechanical components are profoundly influenced by the characteristics of their surface topography [1]. Burnishing, a specialized finishing technique, presents a promising avenue for enhancing machined surfaces' microstructure and surface quality without generating undesirable chips [2,3]. This process involves the application of a cold working pressure that exceeds the yield stress of the workpiece, accomplished by rolling a rigid ball or roller on the surface [4, 5]. It is possible to achieve improved surface characteristics through burnishing, including enhanced surface roughness, hardness, and corrosion resistance [6].

Previous investigations have underscored the significance of optimizing burnishing parameters to simultaneously reduce power consumption and enhance surface finish quality and micro-hardness [7]. Surface roughness emerges as a critical factor among the various surface characteristics affected by burnishing. Experimental observations have revealed an initial decrease in surface roughness with increasing burnishing speed, reaching a minimum value before exhibiting an upward trend [8]. This reduction in surface roughness can be attributed to the plastic deformation of asperities, which is influenced by the larger contact area resulting from an increase in feed rate. However, excessive increments in the feed rate can lead to micro-profile distortion [9]. Furthermore, augmenting the burnishing depth contributes to greater plastic deformation, resulting in lower surface roughness [10, 11].

Another significant surface feature influenced by the burnishing process is out- of-roundness. Elevating the burnishing speed has been found to positively reduce out-of-roundness due to the consequent rise in temperature at the interface between the ball and the workpiece. Increasing temperature induces material softening, mitigating out-of-roundness errors [12]. Conversely, increasing the feed rate while reducing the burnishing time can compromise the effectiveness of the burnishing contact zone, leading to an increase in out-of-roundness [13]. Moreover, while an initial increase in burnishing depth tends to reduce out-of-roundness, further increments can cause the surface layers to excessively harden, potentially resulting in flaking and subsequent increases in out-of-roundness [14].

A wide range of tools were developed for burnishing process. Based on the tool development, it is observed that the burnishing parameters such as force, feed, speed,

number of tool passes, ball diameter and lubrication medium have a greater influence on the surface characteristics of the component [15].

Motivated by the considerations above, the present study aims to investigate the influence of burnishing parameters, specifically tool type, burnishing speed, feed rate, and burnishing depth, on the surface roughness and out-of-roundness of AISI 1035 steel. The experimental approach will utilize the well-established Taguchi and Response Surface Methodology (RSM) techniques, enabling systematic variations of these parameters for a detailed analysis of their effects. The outcomes of this study will contribute to an in-depth understanding of burnishing parameter optimization, facilitating the attainment of superior surface characteristics in mechanical components and ultimately enhancing their precision and functionality.

2. EXPERIMENTAL INVESTIGATION

2.1 Workpieces

The workpiece under investigation was derived from AISI 1035, owing to its carbon content of 0.35 percent by weight. The chemical composition of AISI 1035, including the proportions of its constituent elements, is detailed in Table 1. A carefully prepared specimen was employed for a tensile test to evaluate the material's mechanical properties. This test involved subjecting the specimen to an axial load until failure, enabling the determination of crucial mechanical parameters such as ultimate tensile strength, yield strength, and elongation. The physical and mechanical properties of AISI 1035, encompassing characteristics such as density, thermal conductivity, specific heat capacity, Young's modulus, yield strength, ultimate tensile strength, and elongation, are presented comprehensively in Table 2. These properties are indispensable indicators of the material's response to external forces and ability to withstand mechanical loads.

Table 1. Providing a comprehensive overview of the chemical composition of AISI 1035.

Grade	Chemical Composition %							
	C%	Si%	Mn%	S%	P%	Cr%	Ni%	Cu%
C35	0.34	0.20	0.80	≤0.035	≤0.035	≤0.25	≤0.25	≤0.25

Table 2. Presents a comprehensive compilation of the physical and mechanical properties associated with AISI 1035.

Grade	Density g/cm^3	Tensile Strength (MPa)	Yield Strength (MPa)	Elongation in 100-150 mm (%)	Hardness (HB)
C35	7.85	≥380	≥210	≥25	≤111

The workpieces utilized in the study were prepared using a center lathe, a commonly employed machining tool known for its precision and versatility. The lathe was operated under specific cutting parameters to ensure consistency and reproducibility of the workpiece dimensions. The cutting parameters employed in the lathe operation included a rotational speed of 600 RPM, a cutting feed rate of 0.1 mm/rev, and a cutting depth of 0.1 mm. These parameters were carefully selected to achieve optimal machining conditions while maintaining dimensional accuracy and surface integrity. The workpiece was meticulously constructed per the specifications outlined in Fig. 1. It featured a cylindrical geometry with a diameter of 50 mm and a length of 400 mm. The choice of these dimensions was guided by the requirements of the experimental setup and the need to ensure uniformity among the workpieces. The cylindrical configuration of the workpiece facilitated subsequent processing and allowed for the controlled application of the burnishing process. By adhering to these specific lathe-cutting parameters and constructing the workpiece with precise dimensions, the study aimed to minimize variability and ensure consistency in the subsequent burnishing experiments. This meticulous approach to workpiece preparation is crucial in scientific research, as it lays the foundation for reliable and meaningful results, enabling accurate analysis and interpretation of the effects of burnishing parameters on the material's surface characteristics.

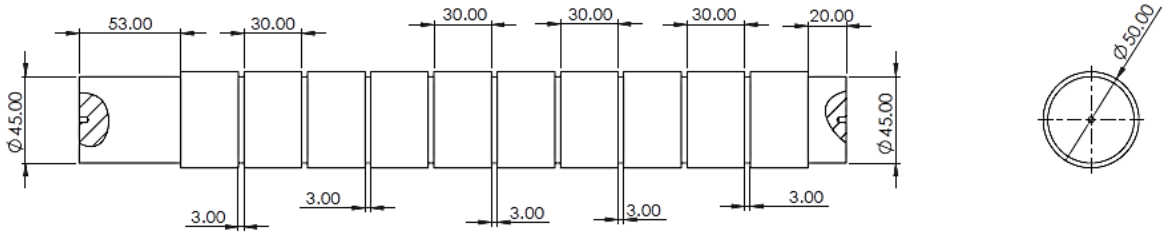

Fig. 1: Workpiece construction showing the workpiece diameter and sectors.

2.2 Tools

For this investigation purpose three types of burnishing tools are used: a purchased rigid tool, a custom-designed spring-assisted burnishing tool, and a pneumatic burnishing tool. As illustrated in Fig. 2, a robust burnishing tool was procured from Taizhou Ke Chi Machinery Company in China, specifically designated with the JC-SQ8R2030 burnishing tool code. The tool was meticulously selected to meet the requirements of the experimental investigation. It comprised an 8 mm tungsten carbide ball, renowned for its exceptional hardness and wear resistance properties. Notably, the tool featured a 30° bent tip configuration, facilitating optimal contact with the workpiece surface during burnishing. Additionally, the tool was equipped with a 20×20 mm tool shank, providing stability and rigidity during operation. The careful selection and procurement of the burnishing tool ensured compatibility with the experimental setup and enabled the precise application of controlled burnishing forces and parameters.

Fig. 2: A rigid burnishing tool was used in this study, with a tungsten carbide ball, 30° bend tip, and 20×20 mm shank.

Figure 3 depicts the custom-designed spring-assisted burnishing tool employed in the present study, specifically tailored to meet the requirements of the investigation. The tool shank, which exhibits a cross-section of 2020 mm, is fabricated from tool steel and has undergone hardening and tempering heat treatments to enhance its mechanical properties. The ball tip, with identical mechanical characteristics to a conventional burnishing tool, is crafted from tungsten carbide and boasts an 8 mm diameter. The tool incorporates a commercially available rectangular cross-section spring with a stiffness of 168 N/mm and a preloaded compression of 2 mm, comprising the mechanism responsible for spring assistance. This spring mechanism, characterized by its inherent spring properties, partially absorbs the applied force during the burnishing process, imparting a narrower range of burnishing forces than the rigid tool paradigm. The spring-assisted burnishing tool offers improved control and precision in applying the burnishing force, ensuring a more consistent and controlled surface treatment process.

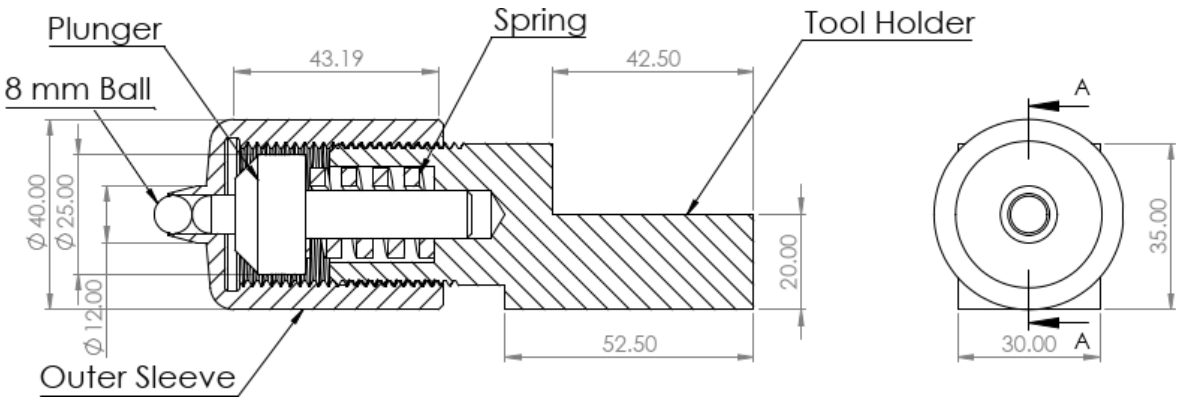

Fig. 3: Spring-assisted burnishing tool designed and manufactured with a 20 x 20 mm tool shank.

The third tool utilized in this comparative analysis was a pneumatic burnishing tool, specifically designed for this research. The tool was equipped with an air-driven motor to enable automated operation and shared the same tool shank and ball tip as the spring-assisted tool. The ball tip, composed of tungsten carbide, had a diameter of 8 mm. Unlike the spring-loaded and rigid tools, the pneumatic tool did not employ a mechanical mechanism for force application. Instead, the pneumatic motor delivered a consistent force, allowing for precise control of the burnishing parameters. The assembly of the pneumatic tool is depicted in Fig. 4. The ball was pressurized with 7 bars of air pressure generated by an air compressor, facilitating the controlled application of force during the burnishing process. Using the pneumatic burnishing tool offered enhanced control and repeatability, enabling accurate and consistent surface treatment.

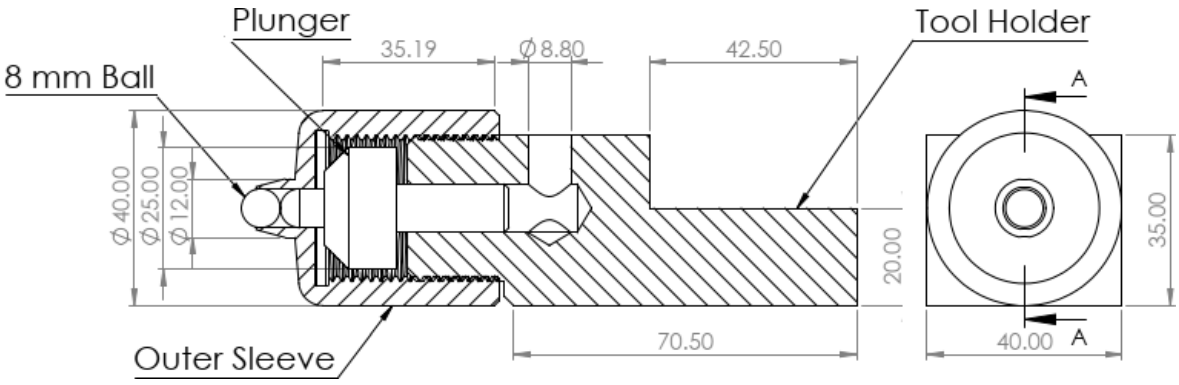

Fig. 4: Pneumatic burnishing tool assembly with automated air-driven motor to precisely control burnishing parameters.

2.3 Testing Procedures and Measurements

This investigation conducted the experiment using the Taguchi experimental test design approach. The Taguchi method was used to conduct 16 experiments per tool, with three quantitative factors, burnishing speed, N (RPM), burnishing feed, S (mm/rev), and tool depth of ball penetration, h (mm), being chosen at four levels. Table 3 displayed the variable levels and Taguchi Array.

Table 3. Study parameters selected for burnishing process.

parameter	Burnishing Speed, N (RPM)	Burnishing Feed, S (mm/rev)	Depth of penetration, h (mm)
1	300	0.09	0.20
2	400	0.10	0.25
3	500	0.11	0.30
4	600	0.12	0.35

Using the Mitutoyo surftest SJ-310, the surface roughness factors (arithmetic average R_a, No. of peaks per centimeter R_{pc}) values were determined. The cut-off length was set at 0.8mm. The workpiece has been separated into three circumferential sections to facilitate the locational measurements. For optimal results, an arithmetic average of three readings was calculated.

Out-of-roundness (O) was measured using the HEXAGON 257 CMM machine, renowned for its precision and accuracy. The test involved the acquisition of 100 data points along the circumference of the specimen, employing a machine with a sensitivity of 0.1 m. A detailed depiction of the obtained measurements, specifically illustrating the deviation from circularity or roundness, is presented in Fig. 5. The study experiments as well as the study outcomes for the different burnishing tools used in this investigation are listed in table 4.

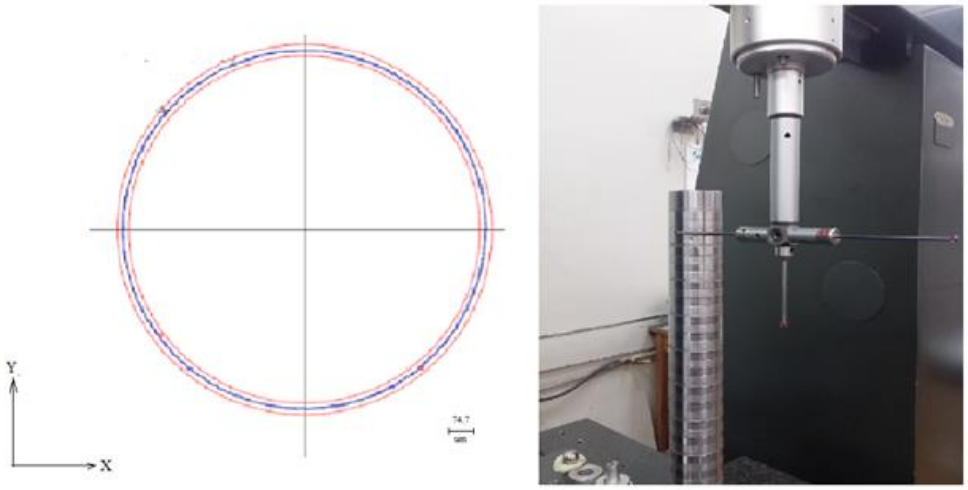

Fig. 5: Out of roundness measurements of the workpiece using CMM machine.

3. RESULTS AND DISCUSSIONS

This study employed the Taguchi technique to determine the optimal burnishing parameters and predict the associated outcomes to minimize surface out-of-roundness and surface roughness. Following Taguchi's approach, a loss function was utilized to quantify the discrepancy between the desired and actual values. Low surface roughness and minimal out-of-roundness are always desirable for optimizing product performance. Thus, the surface response parameters, namely surface roughness, and out-of-roundness, were classified as "smaller is better" type problems. The signal-to-noise ratio (S/N ratio) was computed as η(Ra) and η(OR) in this context.

The computation of the signal-to-noise ratio involved converting the loss function, which is a key step in evaluating the burnishing performance outcomes. The loss function definitions used in this investigation corresponded to the "lower is better" criterion and were applied to n repeated measurements, denoted as y_i. The expressions for the loss functions are as follows:

$$LB_\eta = \left(S/N\right)_{LB} = -10 \log \left[\frac{1}{n}\right] \sum_{i=1}^{n} y_i^2 \qquad (1)$$

Table 4. Taguchi array for L16 design of experiments and study outcomes for different burnishing tools.

No.	N (RPM)	S (mm/rev.)	h (mm)	Rigid Tool			Spring-Assisted Tool			Pneumatic Tool		
				Ra (µm)	Rpc (1/cm)	O (µm)	Ra (µm)	Rpc (1/cm)	O (µm)	Ra (µm)	Rpc (1/cm)	O (µm)
1	300	0.09	0.20	0.22	35.5	11	0.47	66.2	14.9	0.95	123.5	14
2	300	0.10	0.25	0.19	30	8.6	0.46	65.1	15.8	0.83	110.4	15.9
3	300	0.11	0.30	0.18	29.9	8.6	0.43	61.8	16.6	0.84	111.5	16
4	300	0.12	0.35	0.16	26.8	8.4	0.37	55.3	17.2	0.9	118.1	18.8
5	400	0.09	0.25	0.18	29.6	8.9	0.4	58.6	12.9	0.84	111	16.7
6	400	0.10	0.20	0.19	31	10.4	0.43	61.9	11.3	0.78	105	15.6
7	400	0.11	0.35	0.14	25.3	6.3	0.37	55	15.5	0.89	116.9	17.8
8	400	0.12	0.30	0.16	26.2	6.9	0.39	57.5	15.2	0.92	120.2	19.3
9	500	0.09	0.30	0.13	24	7.7	0.41	59.7	16	0.83	110.1	19.4
10	500	0.10	0.35	0.12	23.1	7.3	0.38	56.4	16.5	0.84	111.2	18.9
11	500	0.11	0.20	0.2	31.7	8.9	0.51	70.6	15.6	0.87	114.8	17.7
12	500	0.12	0.25	0.14	26.3	8	0.45	64.1	15.8	0.93	121.3	19.6
13	600	0.09	0.35	0.11	22.1	5.9	0.36	54.2	18.2	0.81	108.2	18.3
14	600	0.10	0.30	0.17	28.5	7.2	0.42	60.8	16.2	0.92	119.8	17.8
15	600	0.11	0.25	0.18	30	7.4	0.5	69.5	15.6	0.82	109.5	18.4
16	600	0.12	0.20	0.19	31.5	9.7	0.51	70.3	14	0.78	105.3	19.5

The primary objective of this study was to optimize the burnishing process through the utilization of the optimization techniques and the application of appropriate loss functions. The aim was to identify the parameter settings that would result in the lowest surface roughness and out-of-roundness, thereby improving the product's overall performance. To achieve this, the Response Surface Methodology (RSM) was employed to develop mathematical models that establish the relationship between burnishing response variables (surface roughness factors and out-of-roundness) and the burnishing parameters for various tool types, including rigid tools, spring tools, and pneumatic tools. These models were developed by utilizing polynomial response surface parameters of the second order and were subjected to evaluation and analysis. The evaluation process involved the utilization of the student's t-test to assess the significance of the process variables and their interactions. This statistical analysis provided insights into the influence of the burnishing parameters on the surface characteristics, allowing for effective optimization of the burnishing process. Table 5 presents a summary of the burnishing parameters considered in this analysis. The careful examination and analysis of the experimental data and the mathematical models developed through the Response Surface Methodology enabled a comprehensive understanding of the relationship between the burnishing response variables and the burnishing parameters. This knowledge is crucial for achieving enhanced surface quality and overall product performance [16,17].

Table 5. Mathematical models for different burnishing responses predicted by RSM method for different burnishing tools.

Tool		Mathematical Models
Rigid Tool	R_a (µm)	0.318 - 0.000569 N + 5.64 S - 1.807 h + 0.000001 N*N - 50.0 S*S - 0.000864 N*h + 16.82 S*h
	Rpc/cm	60.9 - 0.0774 N + 436 S - 220.5 h + 0.000107 N*N - 4687 S*S - 0.0711 N*h + 1907 S*h
	O (µm)	35.2 - 272 S - 56.7 h + 0.000012 N*N + 1125 S*S + 115.0 h*h - 0.0577 N*h
Spring Tool	R_a (µm)	-0.000975 N + 12.99 S + 0.000001 N*N - 57.68 S*S - 1.349 h*h
	Rpc/cm	-0.1029 N + 1692 S + 0.000125 N*N - 7611 S*S - 147.5 h*h
	O (µm)	-0.0564 N + 213.3 S + 96.9 h + 0.000061 N*N - 739 S*h
Pneumatic Tool	R_a (µm)	4.22 - 0.001420 N - 37.5 S - 9.61 h + 106 S*S + 0.00580 N*h + 68.0 S*h
	Rpc/cm	477 - 0.1567 N - 4057 S - 1040 h + 11625 S*S + 0.637 N*h + 7305 S*h
	O (µm)	42.1 + 0.0616 N - 943 S + 40.4 h - 0.000039 N*N + 4687 S*S - 0.0643 N*h

To determine the best ball burnishing process settings, single response optimization was employed to decrease surface roughness factors and out-of-roundness while maximizing surface hardness individually. The optimum influence of ball burnishing process parameters, such as rotational speed, burnishing feed, and penetration depth, was determined by plotting surface roughness factors and out-of-roundness main effect plots (MEP) using Minitab 21 software. The signal-to-noise (S/N) ratio quality characteristics of surface roughness factors and surface out-of-roundness were calculated to assess the experimental results, following the "the smaller, the better" approach.

The main effect plots for each response studied in this investigation were presented in Fig. 6 to 8 for rigid, spring, and pneumatic tools, respectively. The S/N ratio was maximized according to the Taguchi method to identify the optimal cutting condition. Table 6 displays the optimum combination of input burnishing parameters leading to the best results for each response across all burnishing tools. For instance, the minimum surface roughness generated by the rigid tool could be obtained at a burnishing speed of 500 rpm, a feed rate of 0.09 mm/rev, and a penetration depth of 0.35 mm. Similarly, the minimum surface roughness generated by the pneumatic tool could be achieved at a burnishing speed of 600 rpm, a feed rate of 0.1 mm/rev, and a depth of penetration of 0.2 mm.

Regarding out-of-roundness, the minimum value generated by the rigid tool could be obtained at a burnishing speed of 600 rpm, a feed rate of 0.11 mm/rev, and a penetration depth of 0.35 mm. Similarly, the minimum out-of-roundness generated by the spring tool could be achieved at a burnishing speed of 400 rpm, a feed rate of 0.1 mm/rev, and a depth of penetration of 0.2 mm. These optimized parameter combinations were determined using the Taguchi method, ensuring superior burnishing outcomes for the respective responses and tool types.

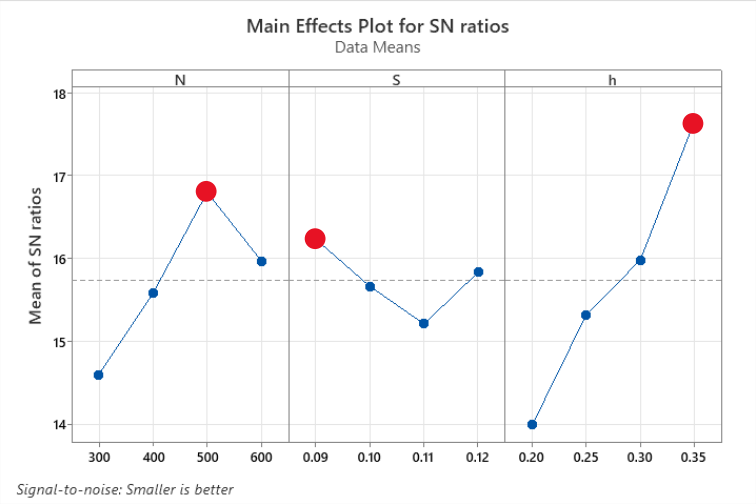

(a)

(b)

(c)

Fig. 6: Main effect Plot for S/N ratio of studied responses for rigid tool for, (a) Ra, (b) Rpc, (c) O.

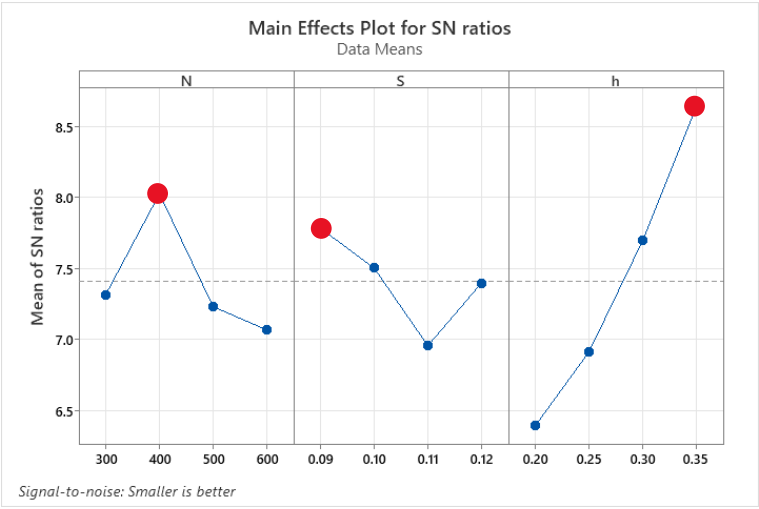

(a)

(b)

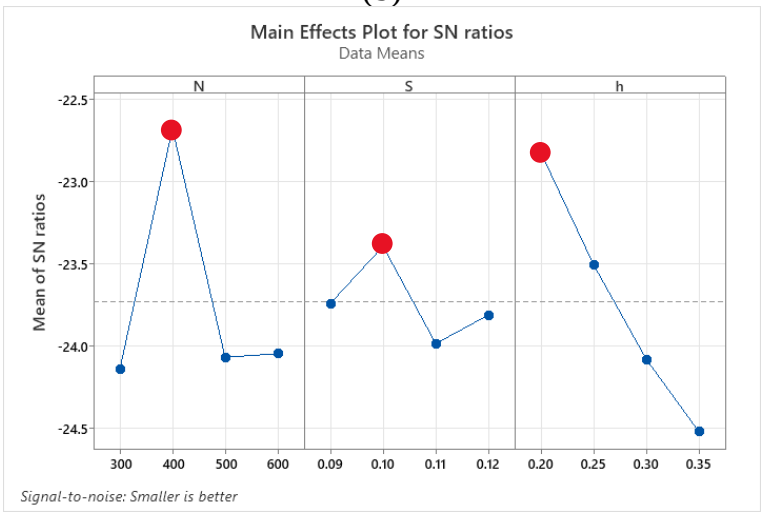

(c)

Fig. 7: Main effect Plot for S/N ratio of studied responses for spring tool for, (a) Ra, (b) Rpc, (c) O.

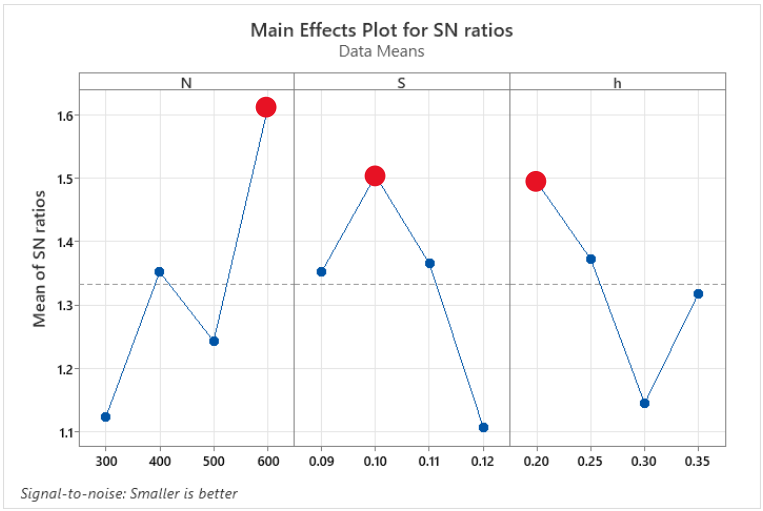

(a)

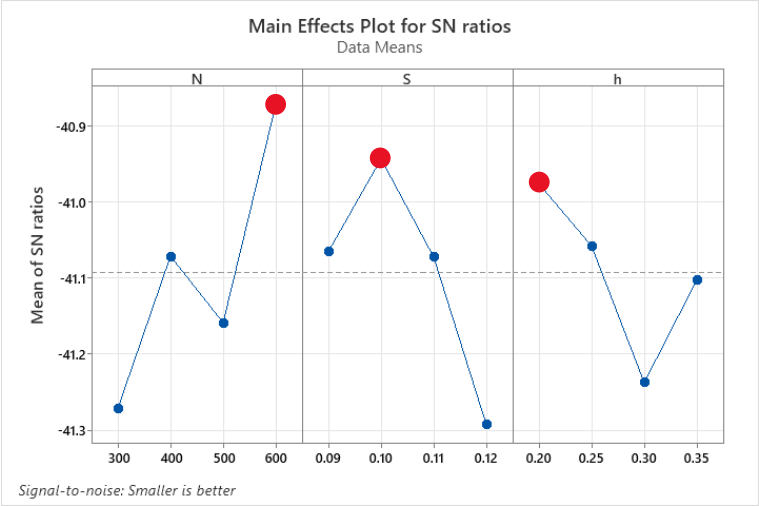

(b)

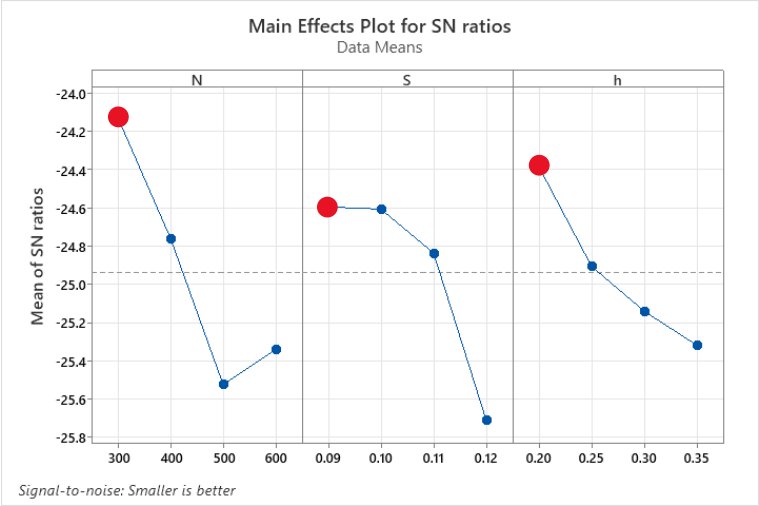

(c)

Fig. 8: Main effect Plot for S/N ratio of studied responses for pneumatic tool for, (a) Ra, (b) Rpc, (c) O.

Table 6. Optimum ball burnishing parameters according to Taguchi method for rigid, spring, and pneumatic tools, respectively.

Responses	Rigid Tool			Spring Tool			Pneumatic Tool		
	N	S	h	N	S	h	N	S	h
	RPM	mm/rev	mm	RPM	mm/rev	mm	RPM	mm/rev	mm
Ra	500	0.09	0.35	400	0.09	0.35	600	0.1	0.2
Rpc	500	0.09	0.35	400	0.09	0.35	600	0.1	0.2
O	600	0.11	0.35	400	0.1	0.2	300	0.09	0.2

The main objective of this investigation was to optimize the surface characteristics of the ball burnishing process by manipulating the specified

parameters. Response Surface Methodology, a sequential technique known for its efficiency in approaching the optimal region and effectively illustrating the response, was employed. The effectiveness of the Response Surface Methodology in optimizing the burnishing process parameters for surface roughness and out-of-roundness has been well- established. Single response optimization was conducted to explore input parameters' impact on individual responses' desirability. Numerical optimization techniques were employed to identify the point that maximizes the desirability function.

The optimal combination of input burnishing parameters leading to the best results for each response of both alloys is presented in Fig. 9 to 11 as well as Table 7. For instance, the minimum surface roughness generated by the rigid tool was obtained at a burnishing speed of 496.9697 rpm, a feed rate of 0.09 mm/rev, and a penetration depth of 0.35 mm. Similarly, the minimum surface roughness generated by the spring tool was achieved at a burnishing speed of 451.5152 rpm, a feed rate of 0.12 mm/rev, and a penetration depth of 0.35 mm.

On the other hand, minimum out-of-roundness generated by the rigid tool can be obtained at a burnishing speed of 600 rpm, feed rate of 0.12 mm/rev, and penetration depth of 0.35 mm. However, minimum out-of-roundness generated by the pneumatic tool can be obtained at a burnishing speed of 300 rpm, feed of 0.1006 mm/rev, and penetration depth of 0.2 mm.

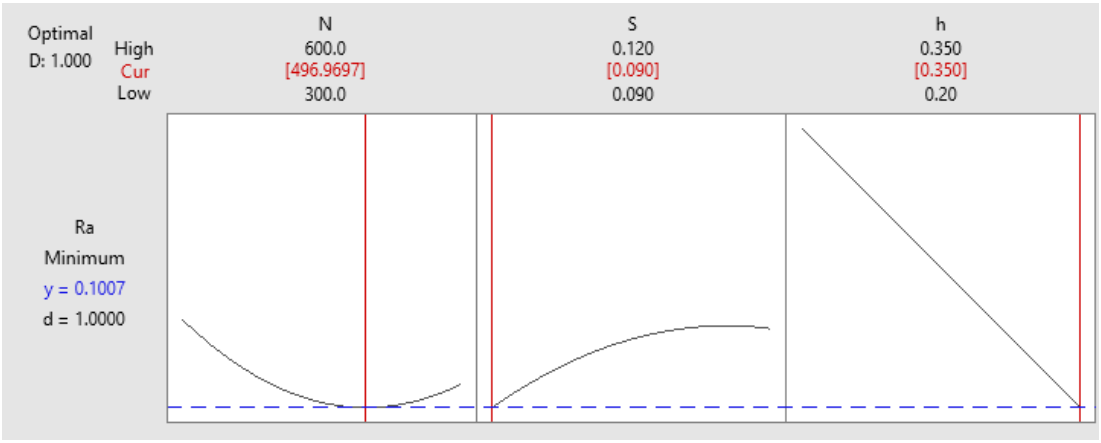

(a)

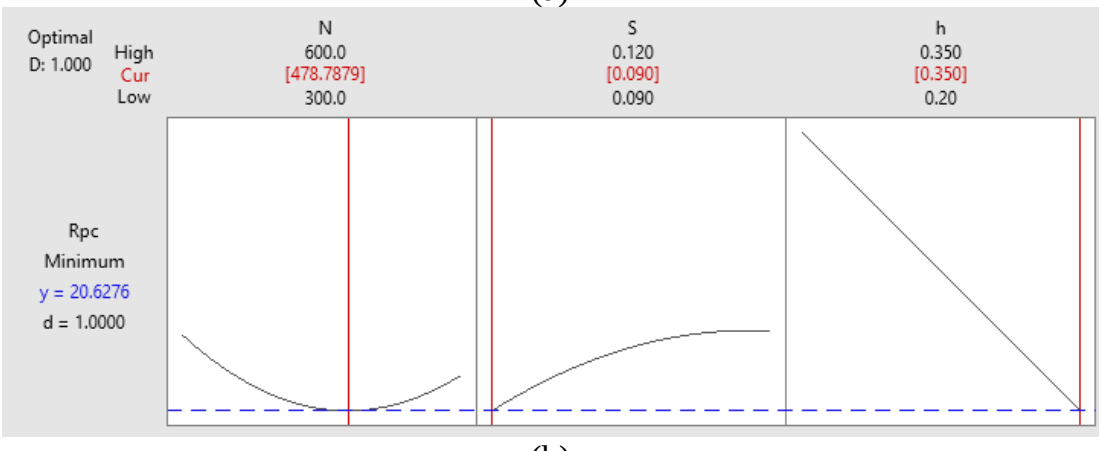

(b)

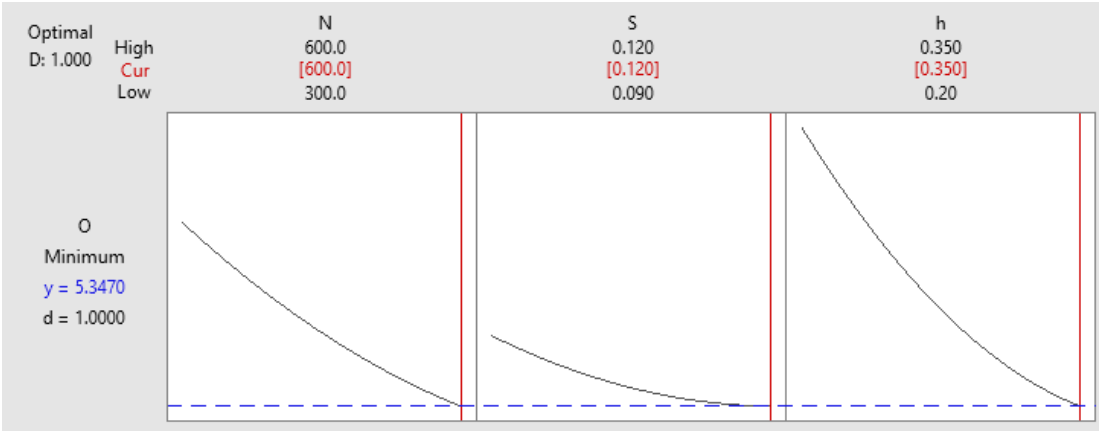

(c)

Fig. 9: Selected optimum parameters for different responses of rigid tool for, (a) Ra, (b) Rpc, (c) O.

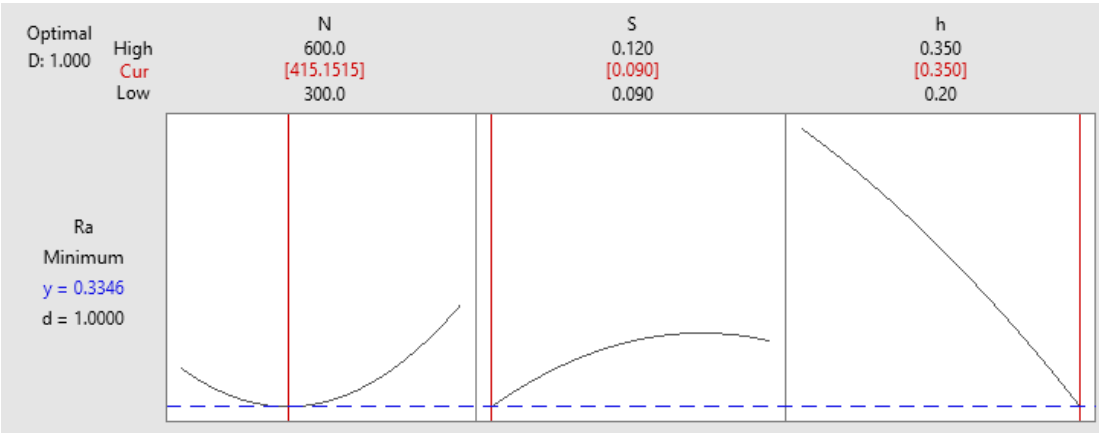

(a)

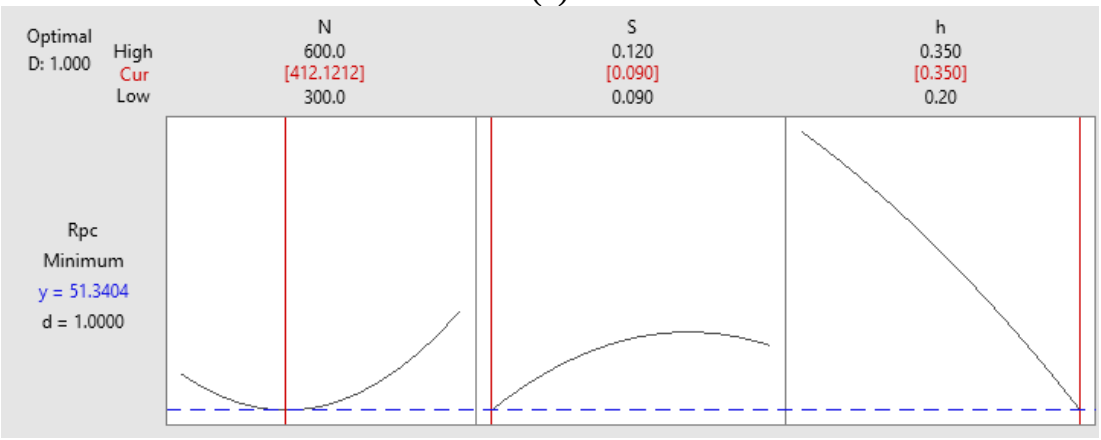

(b)

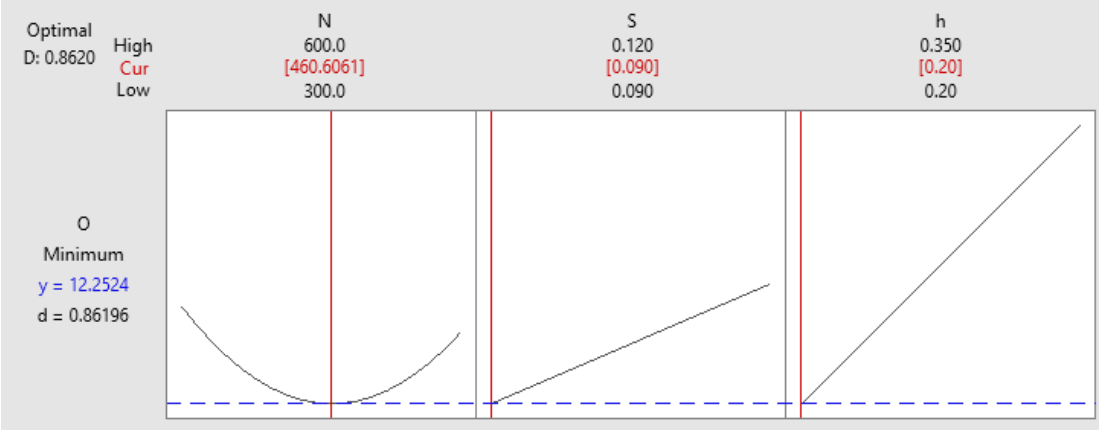

(c)

Fig. 10: Selected optimum parameters for different responses of spring tool for, (a) Ra, (b) Rpc, (c) O.

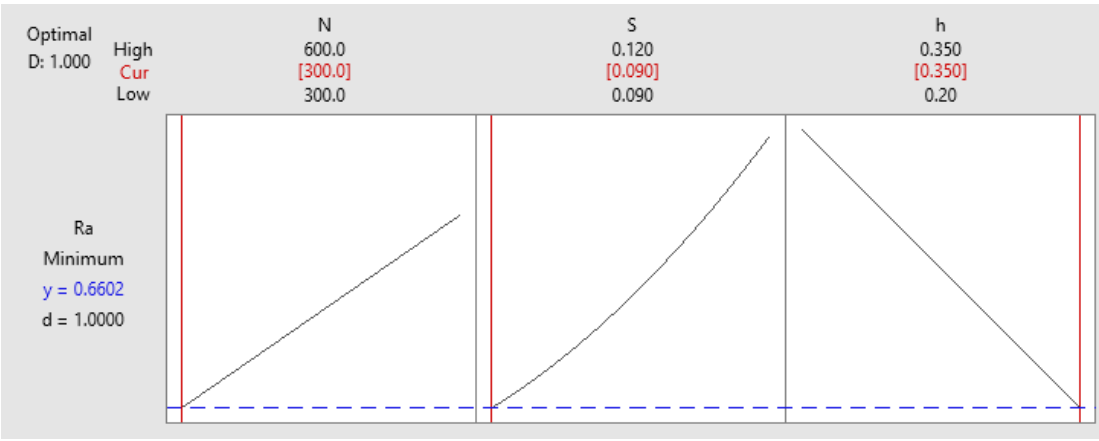

(a)

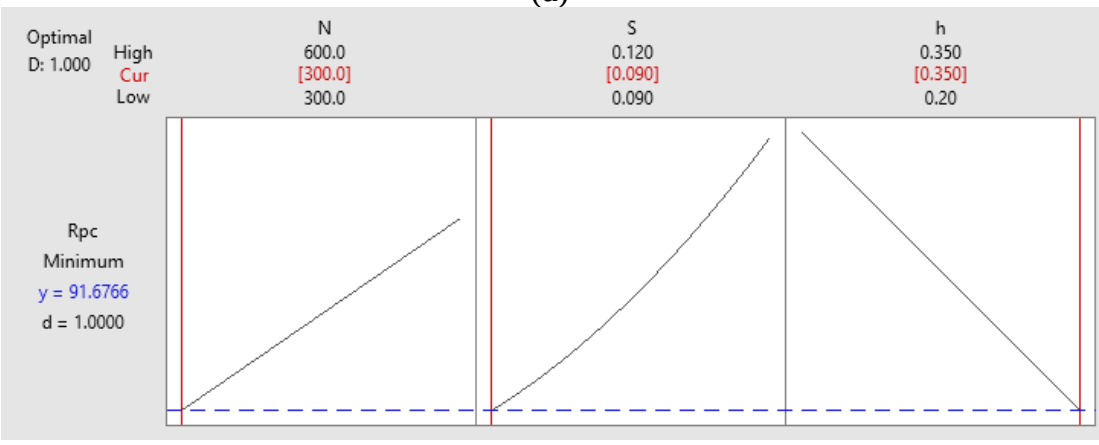

(b)

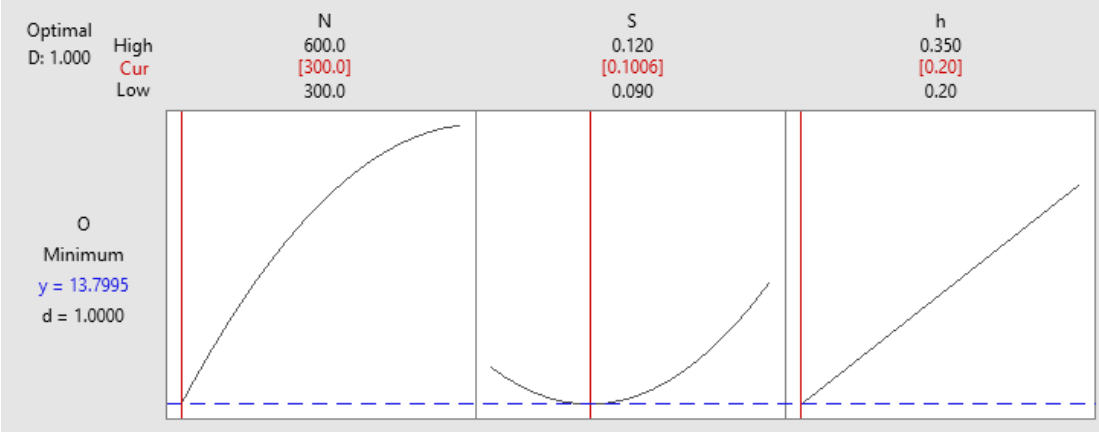

(c)

Fig. 11: Selected optimum parameters for different responses of pneumatic tool for, (a) Ra, (b) Rpc, (c) O.

Table 7. Optimum ball burnishing parameters according to RSM method for rigid, spring, and pneumatic tools, respectively.

Responses	Rigid Tool			Spring Tool			Pneumatic Tool		
	N	S	h	N	S	h	N	S	h
	RPM	mm/rev	mm	RPM	mm/rev	mm	RPM	mm/rev	mm
Ra	496.97	0.09	0.35	415.15	0.09	0.35	300	0.09	0.35
Rpc	478.79	0.09	0.35	412.12	0.09	0.35	300	0.09	0.35
O	600	0.12	0.35	460.61	0.09	0.2	300	0.1006	0.2

Predicting the burnishing results in accordance with the experimental method applied is an important benefit of using experimental test design techniques. A comparison between the experimental and predicted findings using Taguchi and RSM approaches is done with reference to Fig. 12 to 14. Using Taguchi and RSM experimental design approaches, the experimental findings of the surface quality indicators (Ra, Rpc, and O) of steel 50 bars burnished by various tools utilized in this study are compared with the statistical values expected. The figures indicate that there is little deviation between the experimental and predicted data, indicating a modest expected error between the various methods. This suggests that both methods are efficient in optimizing the burnishing procedure and predicting the burnishing outcomes.

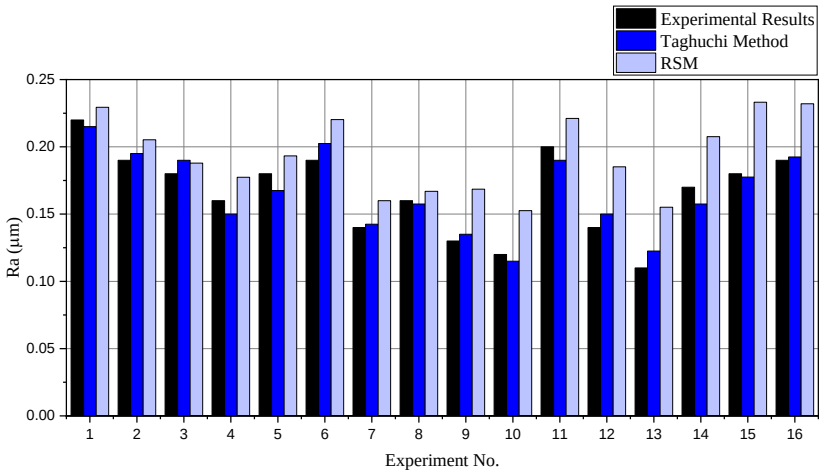

(a)

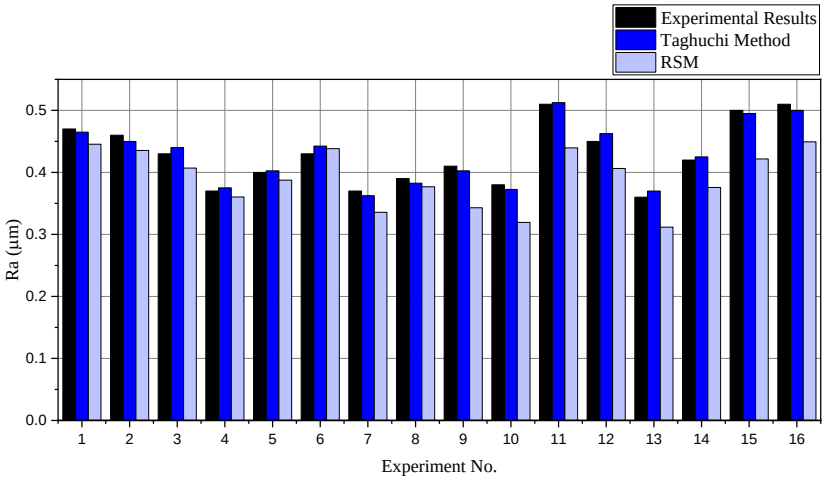

(b)

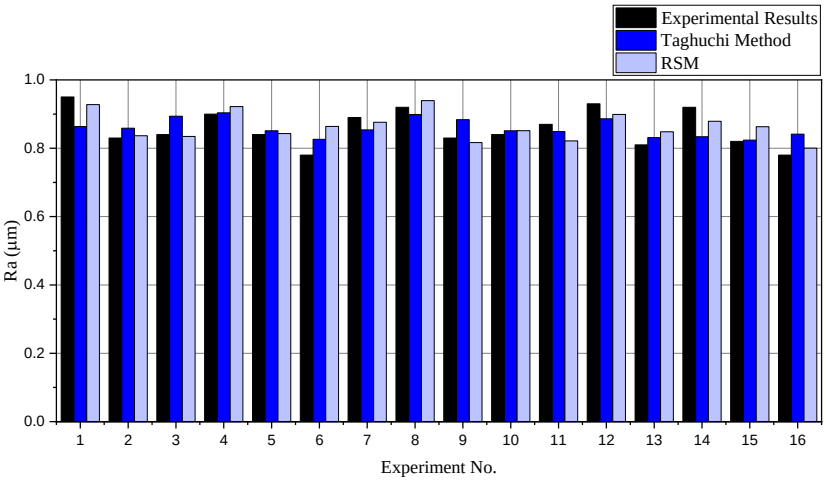

(c)

Fig. 12: Comparison Between Experimental and Predicted Results of Taguchi and RSM Methods for Average Surface Roughness for, (a) rigid tool, (b) spring tool, (c) pneumatic tool.

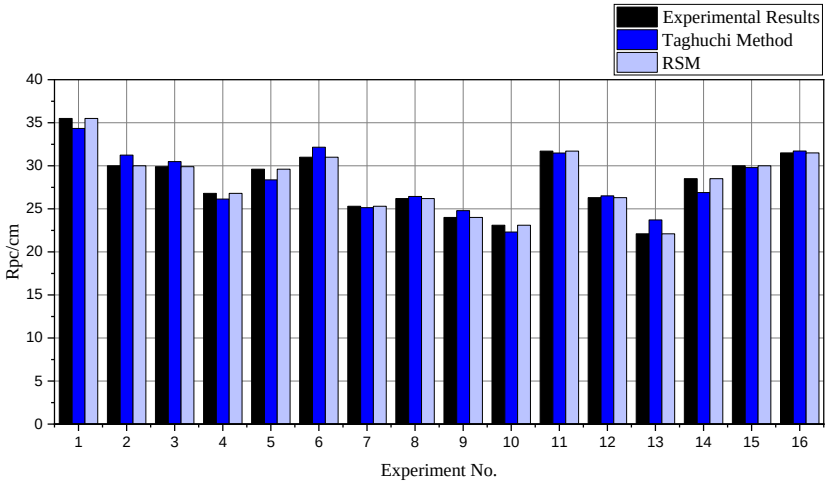

(a)

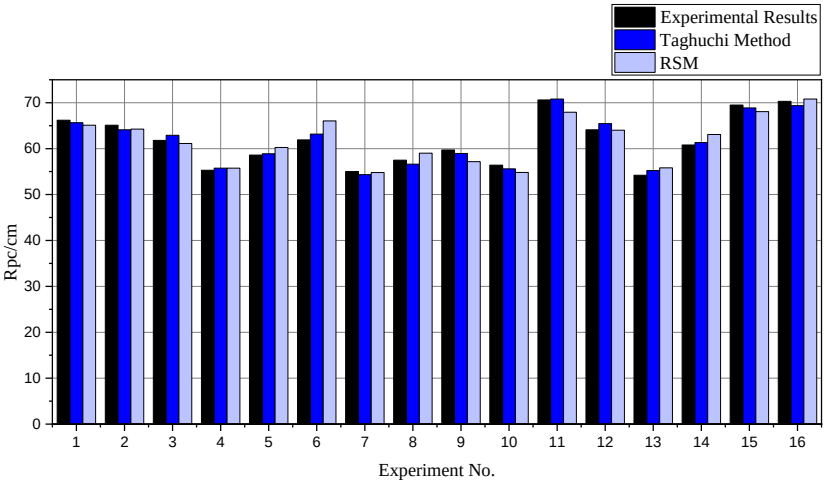

(b)

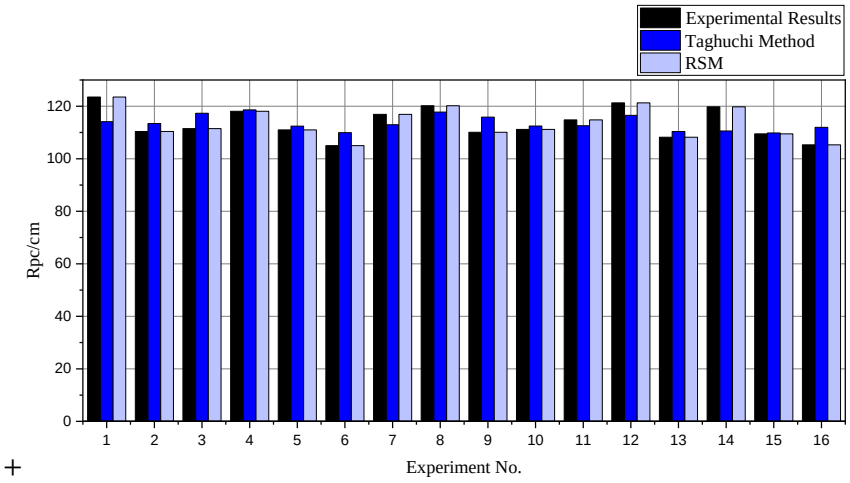

(c)

Fig. 13: Comparison Between Experimental and Predicted Results of Taguchi and RSM Methods for No. of Peaks Per Centimeter for, (a) rigid tool, (b) spring tool, (c) pneumatic tool.

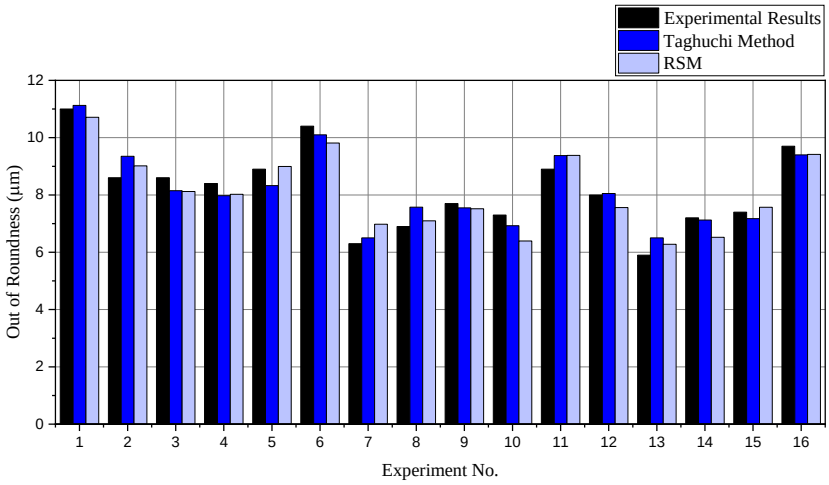

(a)

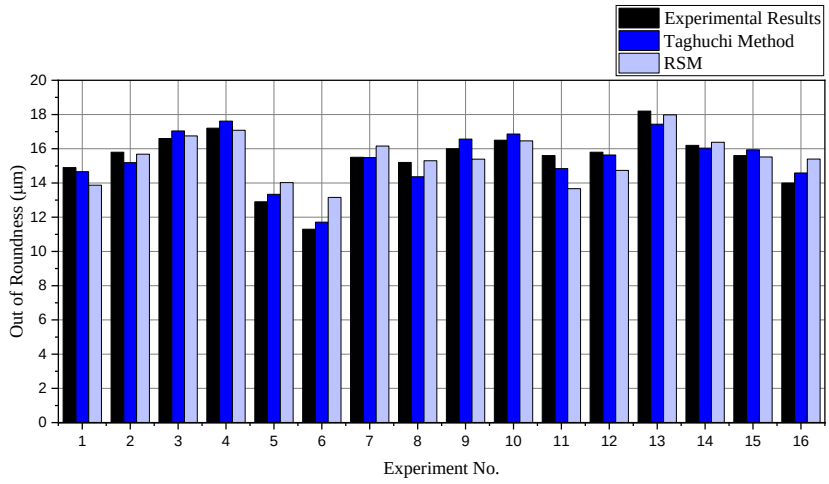

(b)

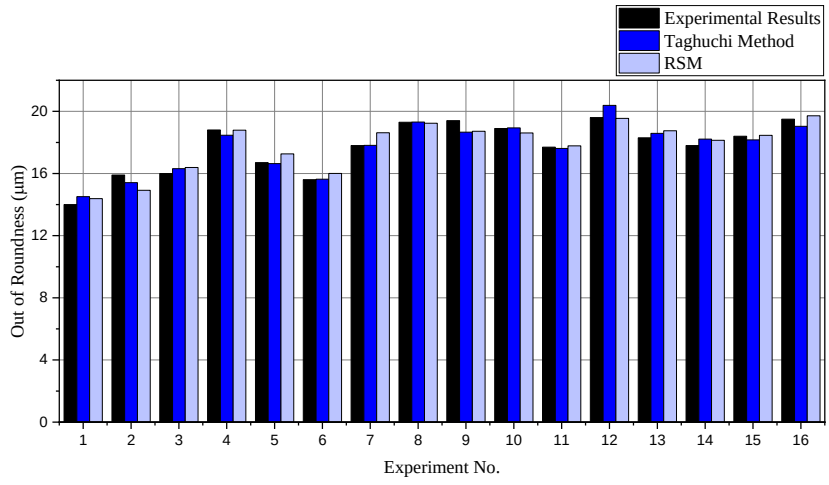

(c)

Fig. 14: Comparison Between Experimental and Predicted Results of Taguchi and RSM Methods for Out-of-Roundness for, (a) rigid tool, (b) spring tool, (c) pneumatic tool.

Determining the best prediction with the smallest possible margin of error utilizing Taguchi and RSM approaches is done through percentage error analysis. The expected error was determined using the formula below:

$$Percentage\ Error\ (\%) = \left|\frac{Experimental\ Result - Predicted\ Result}{Experimental\ Result}\right| \times 100 \qquad (2)$$

Using rigid, spring, and pneumatic burnishing tools, Figure 15 shows the error analysis for the average surface roughness No. (Ra). The figure illustrates that, in most design points, the percentage error determined by the Taguchi technique is less than that determined by the RSM method for both rigid and spring tools. In most design points, the predicted error for the pneumatic tool using the Taguchi approach is greater than the predicted error for the RSM method. Using the RSM approach, the highest error is 42% in a single location, whereas the Taguchi method yields a maximum error of 12%.

Figure 16 compares the predicted errors for the number of peaks per centimeter (Rpc) using different approaches. In most design points for both rigid and pneumatic tools, the expected error calculated by the Taguchi approach is greater than the predicted error using the RSM method, while in most design points the predicted error calculated by the RSM method is greater than the predicted error using the Taguchi method. When the RSM approach is applied, the maximum error is 8.5%; when the Taguchi method is employed, the maximum error is 7.25%.

Using the three burnishing tools developed mainly for this study, the estimated error for out-of-roundness using the Taguchi technique is less than the predicted error for most design points using the RSM method. Figure 17 illustrates the error analysis for out-of-roundness using all three burnishing tools. When applying the Taguchi technique, the maximum error is 10.25%, however, a maximum error of 16.5% occurs when applying the RSM approach.

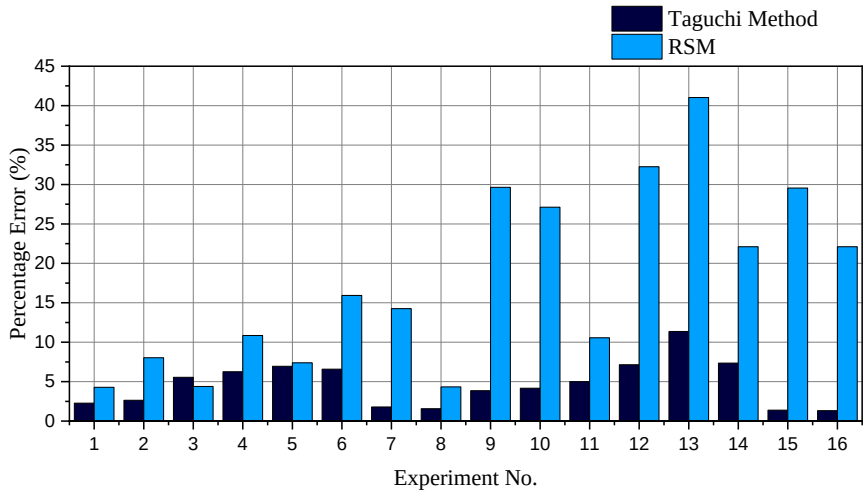

(a)

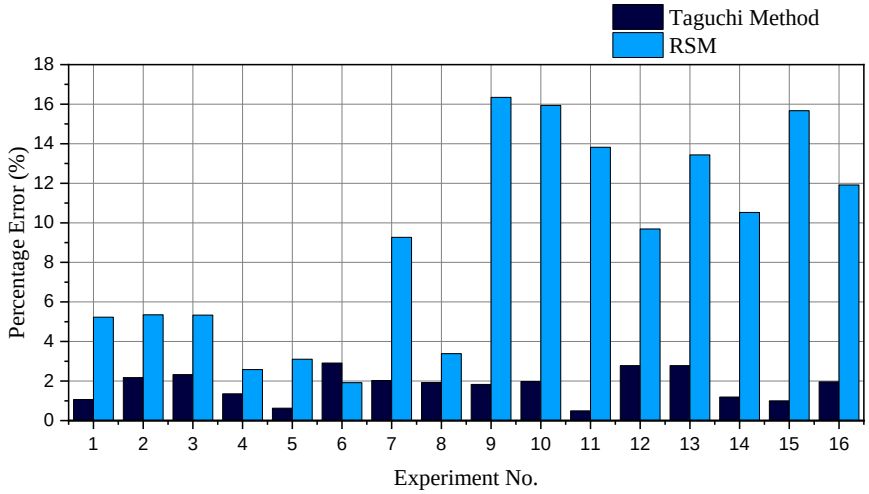

(b)

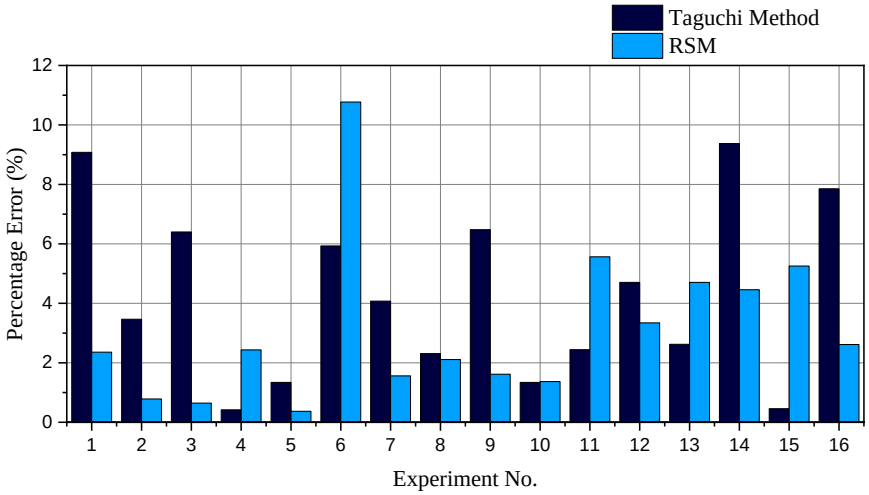

(c)

Fig. 15: Comparison Between Percentage Error of Taguchi and RSM Methods for Average Surface Roughness for, (a) rigid tool, (b) spring tool, (c) pneumatic tool.

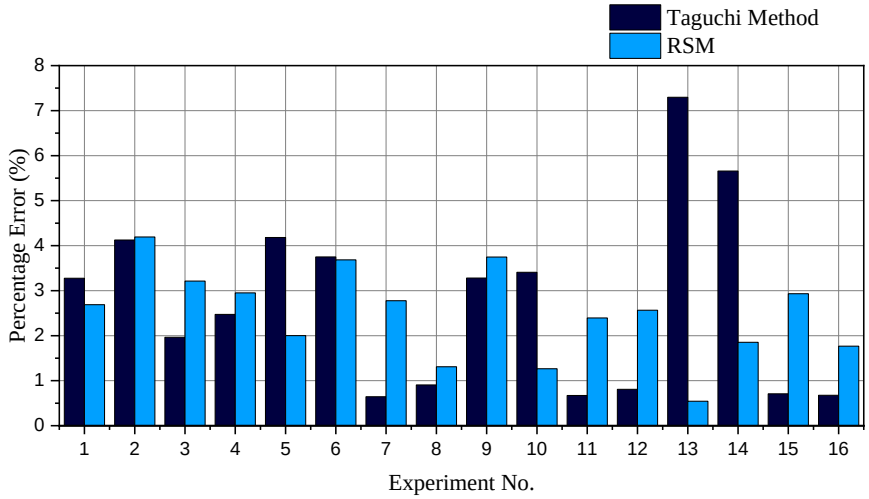

(a)

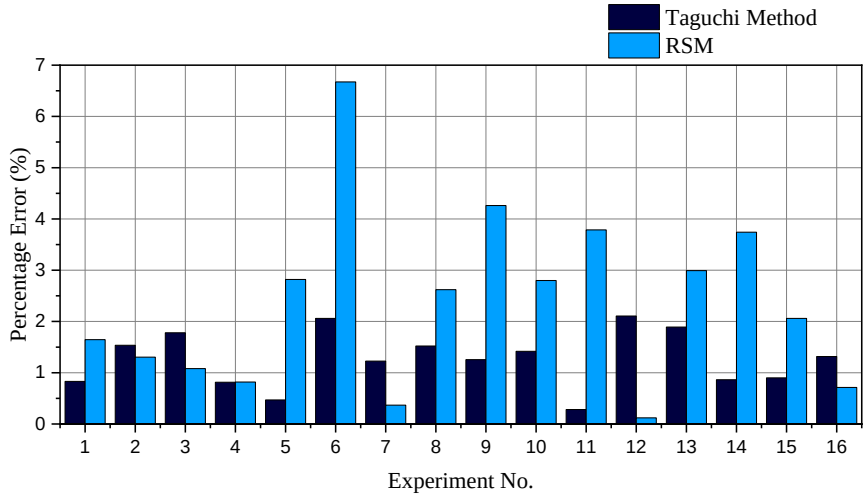

(b)

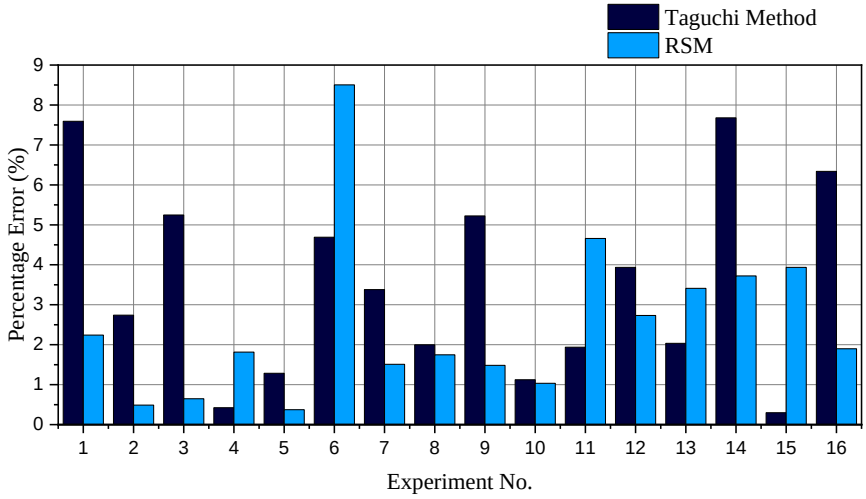

(c)

Fig. 16: Comparison Between Percentage Error of Taguchi and RSM Methods for No. of Peaks Per Centimeter for, (a) rigid tool, (b) spring tool, (c) pneumatic tool.

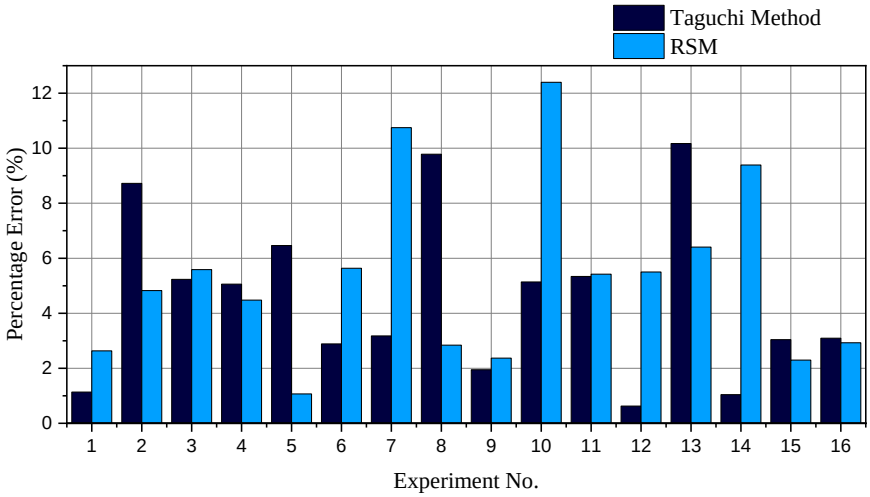

(a)

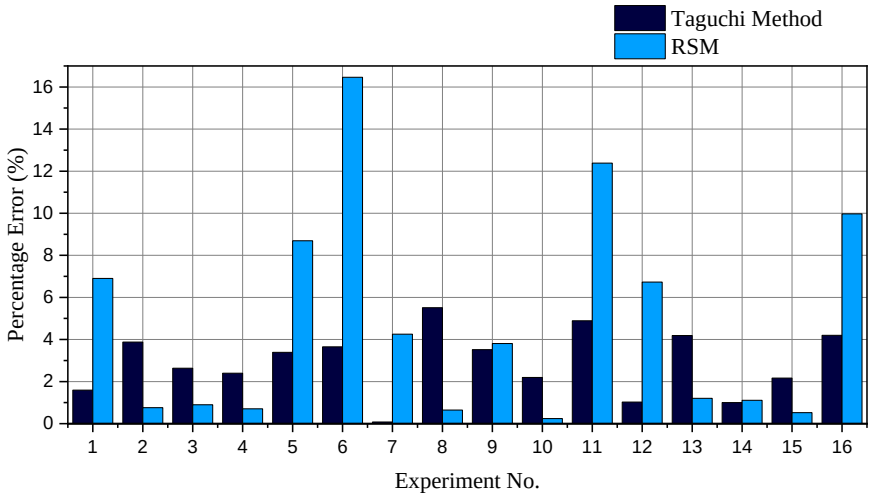

(b)

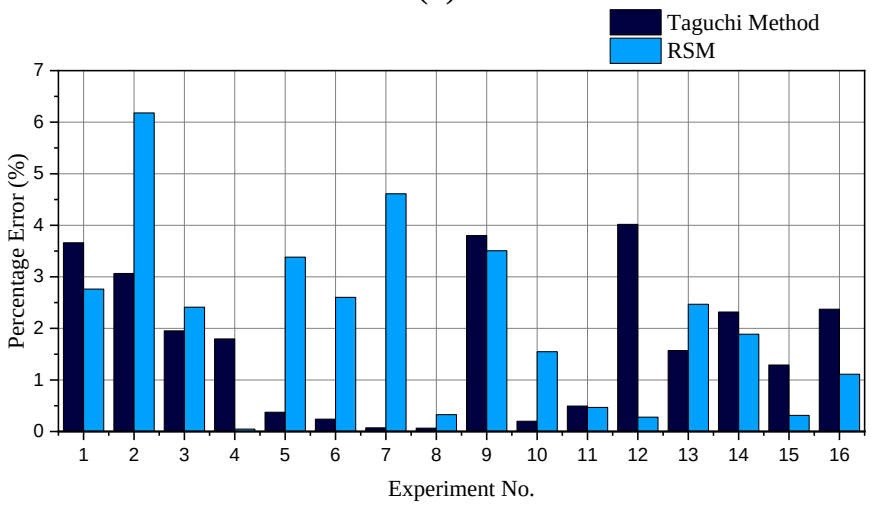

(c)

Fig. 17: Comparison Between Percentage Error of Taguchi and RSM Methods for Out-of-Roundness for, (a) rigid tool, (b) spring tool, (c) pneumatic tool.

4. CONCLUSIONS

In conclusion, this research focused on optimizing ball burnishing process parameters using the Taguchi and Response Surface Methodology (RSM) approaches. The ball burnishing process is a crucial and contemporary surface finishing technique. Three distinct tools were designed and employed in this study, with a Taguchi L16 matrix utilized for the experiments. Surface roughness and out-of-roundness measurements were conducted, and the results were analyzed using the Taguchi and RSM methods. According to experimental observations and statistical analysis this research concluded that:

- When applying the Taguchi method, the rigid tool's minimum surface roughness was achieved at a burnishing speed of 500 rpm, a feed rate of 0.09 mm/rev, and a penetration depth of 0.35 mm, respectively.

- For the pneumatic tool, the minimum surface roughness was obtained at a burnishing speed of 600 rpm, a feed rate of 0.1 mm/rev, and a penetration depth of 0.2 mm.
- Regarding out-of-roundness, the rigid tool achieved minimum values at a burnishing speed of 600 rpm, a feed rate of 0.11 mm/rev, and a penetration depth of 0.35 mm.
- For the pneumatic tool, the minimum value was yielded at a burnishing speed of 300 rpm, a feed rate of 0.09 mm/rev, and a depth of penetration of 0.2 mm.
- The RSM method revealed that the minimum surface roughness generated by the rigid tool could be achieved at a burnishing speed of 496.9697 rpm, a feed rate of 0.09 mm/rev, and a penetration depth of 0.35 mm.
- In the case of the spring tool, the minimum surface roughness was attained at a burnishing speed of 451.5152 rpm, a feed rate of 0.12 mm/rev, and a penetration depth of 0.35 mm.
- Regarding out-of-roundness, the rigid tool yielded the minimum values at a burnishing speed of 600 rpm, a feed rate of 0.12 mm/rev, and a penetration depth of 0.35 mm.
- For the pneumatic tool, the minimum out-of-roundness was achieved at a burnishing speed of 300 rpm, a feed rate of 0.1006 mm/rev, and a penetration depth of 0.2 mm.

REFERENCES

[1] K. A. Prasad and M. R. S. John, “Optimization of external roller burnishing process on magnesium silicon carbide metal matrix composite using response surface methodology,” J. Brazilian Soc. Mech. Sci. Eng., vol. 43, no. 7, pp. 1–12, 2021.

[2] T. A. El-Taweel and M. H. El-Axir, “Analysis and optimization of the ball burnishing process through the Taguchi technique,” Int. J. Adv. Manuf. Technol., vol. 41, no. 3–4, pp. 301–310, 2009.

[3] L. Prabhu, S. Krishnamoorthi, M. A. Akbar, P. Mubashir, and P. Prashob, “Design and fabrication of ball burnishing tool for surface finish,” IOP Conf. Ser. Mater. Sci. Eng., vol. 993, no. 1, 2020.

[4] F. Gharbi, S. Sghaier, K. J. Al-Fadhalah, and T. Benameur, “Effect of ball burnishing process on the surface quality and microstructure properties of aisi 1010 steel plates,” J. Mater. Eng. Perform., vol. 20, no. 6, pp. 903–910, 2011.

[5] C. Priyadarsini, V. S. N. V. Ramana, K. A. Prabha, and S. Swetha, “A review on ball, roller, low plasticity burnishing process,” Mater. Today Proc., vol. 18, pp. 5087–5099, 2019.

[6] G. Rotella, S. Caruso, A. Del Prete, and L. Filice, “Prediction of surface integrity parameters in roller burnishing of ti6al4v,” Metals (Basel)., vol. 10, no. 12, pp. 1–17, 2020.

[7] T. T. Nguyen and M. T. Le, “Optimization of the internal roller burnishing process for energy reduction and surface properties,” Stroj. Vestnik/Journal Mech. Eng., vol. 67, no. 4, pp. 167–179, 2021.

[8] M. Fattouh, M. H. El-Axir, and S. M. Serage, “Investigations into the burnishing of external cylindrical surfaces of 70 30 Cu-Zn alloy,” Wear, vol. 127, no. 2, pp. 123–137, 1988.

[9] V. Kurkute and S. T. Chavan, “Modeling and Optimization of surface roughness and microhardness for roller burnishing process using response surface methodology for Aluminum 63400 alloy,” Procedia Manuf., vol. 20, pp. 542–547, 2018.

[10] T. T. Nguyen, L. H. Cao, X. P. Dang, T. A. Nguyen, and Q. H. Trinh, “Multi-objective optimization of the flat burnishing process for energy efficiency and surface characteristics,” Mater. Manuf. Process., vol. 34, no. 16, pp. 1888–1901, 2019.

[11] M. R. S. John and B. K. Vinayagam, “Optimization of nonlinear characteristics of ball burnishing process using Sugeno fuzzy neural system,” J. Brazilian Soc. Mech. Sci. Eng., vol. 36, no. 1, pp. 101–109, 2014.

[12] M. R. S. John, A. W. Wilson, A. P. Bhardwaj, A. Abraham, and B. K. Vinayagam, “An investigation of ball burnishing process on CNC lathe using finite element analysis,” Simul. Model. Pract. Theory, vol. 62, pp. 88–101, 2016.

[13] M. Boozarpoor, M. Elyasi, and M. Hosseinzadeh, “An investigation of the surface quality of burnished AISI 4340 steel,” Proc. Inst. Mech. Eng. Part E J. Process Mech. Eng., vol. 232, no. 3, pp. 299–313, 2018.

[14] M. H. El-Axir, O. M. Othman, and A. M. Abodiena, “Improvements in out-of-roundness and microhardness of inner surfaces by internal ball burnishing process,” J. Mater. Process. Technol., vol. 196, no. 1–3, pp. 120–128, 2008.

[15] A. Raza and S. Kumar, “Tribology International A critical review of tool design in burnishing process,” Tribol. Int., vol. 174, no. January, pp. 1–20, 2022.

[16] Li, Feng Lei, et al, "Analytical prediction and experimental verification of surface roughness during the burnishing process," Int. J. Mach. Tools Manuf., vol. 62, pp. 67-75, 2012.

[17] K. A. Patel and P. K. Brahmbhatt, “A comparative study of the RSM and ANN models for predicting surface roughness in roller burnishing,” Proc. Technol., vol. 23, pp. 391–397, 2016.